EPR of Mn^{2+}-doped single crystals of $ZnK_2(SO_4)_2 \cdot 6H_2O$ and $NiK_2(SO_4)_2 \cdot 6H_2O$: Mn^{2+}-Ni^{2+} exchange constant

Sushil K. Misra and Mojtaba Kahrizi

Physics Department, Concordia University, 1455 de Maisonneuve Boulevard West,

Montreal, Quebec H3G 1M8, Canada

(Received 22 June 1983)

X-band EPR measurements on Mn^{2+}-doped single isostructural crystals of diagmagnetic zinc potassium sulfate hexahydrate and paramagnetic nickel potassium sulfate hexahydrate have been made at room, liquid-nitrogren, and liquid-helium temperatures. To avoid the demagnetization effects, a spherical-shaped sample was used for the paramagnetic lattice. The spin-Hamiltonian parameters were evaluated using a least-squares fitting method, simultaneously fitting all resonant line positions obtained for several orientations of the external magnetic field. Using the *g* shift in the paramagnetic host, from that in the isostructural diamagnetic host, the Mn^{2+}-Ni^{2+} exchange constant has been estimated.

I. INTRODUCTION

EPR measurements on a Mn^{2+}-doped single crystal of zinc potassium sulfate hexahydrate, $ZnK_2(SO_4)_2 \cdot 6H_2O$ (hereafter ZPSH), have been reported by Kasthurirengan and Navalgund[1] (at room temperature only), while those on Mn^{2+}-doped nickel potassium sulfate hexahydrate, $NiK_2(SO_4)_2 \cdot 6H_2O$ (hereafter NPSH), have been reported by Misra and Jalochowski[2] (from room down to liquid-helium temperature). The spin-Hamiltonian parameters (ignoring the fourth-order ones) as reported in Ref. 1 were evaluated from perturbation theory by use of only the resonant line positions obtained for the external magnetic field orientation along the *Z* and *X* axes; further, these measurements were confined to room temperature only. In Ref. 2, while the parameters were rigorously evaluated by use of a least-squares fitting procedure,[3] the shape of the host crystal used was arbitrary, thus being susceptible to demagnetization effects at low temperatures.

Paramagnetic lattices become magnetized at low temperatures, and it is shown by Kittel[4] that in these crystals, for axial symmetry, the observed *g* factor g_{obs} gets shifted from its value *g* in the corresponding isostructural diamagnetic lattice by an amount $[(4\pi/3) - N_z]1.5M/H_0$, where N_z is the demagnetization factor along the axis of symmetry, *M* is the magnetization, and H_0 is the external magnetic field intensity. (N_z is $4\pi/3$ for a spherical sample.) Thus, in order to eliminate this shift due to the demagnetization effect, one should use spherical paramagnetic host crystals. However, there is another *g* shift experienced in paramagnetic lattices, i.e., that due to the exchange interaction between the host paramagnetic ions and the guest paramagnetic ion (for details see Sec. II). Thus for a Mn^{2+}-doped NPSH crystal, for a spherical sample, the *g* shift at low temperatures would depend only upon the Mn^{2+}-Ni^{2+} exchange interaction.

Recently, a rigorous technique using the least-squares fitting procedure, specifically applicable to the electron-nuclear spin-coupled system, e.g., that of a Mn^{2+} ion, has been proposed.[5]

It is the purpose of the present paper to report detailed *X*-band EPR measurements on Mn^{2+}-doped single crystals of ZPSH and NPSH (spherical shape) at room, liquid-nitrogen, and liquid-helium temperatures. From a compar-

ison of the *g* values as found in the two hosts at liquid-helium temperature, the Mn^{2+}-Ni^{2+} exchange-interaction constant has been estimated. Section II deals with the theory of the shift of *g* value due to the presence of paramagnetic host ions, while the crystal structure and sample preparation are given in Sec. III. The resulting values of the spin-Hamiltonian parameters and the Mn^{2+}-Ni^{2+} exchange-interaction constant are discussed in Sec. IV. Linewidth behavior is discussed in Sec. V.

II. *g* SHIFT

The shift of the *g* value due to the presence of paramagnetic host ions is caused by the exchange interaction between the guest and host paramagnetic ions, i.e., Mn^{2+} and Ni^{2+} in the present case. As a result of the polarization effect of the external field, magnetic moments are induced on the paramagnetic host ions. These magnetic moments interact with the guest Mn^{2+} ion, thus causing the presence of an internal field, resulting in the shift of resonance, equivalent to that in the *g* factor.[6-9]

Assuming a pairwise exchange interaction between a Mn^{2+} ion with its nearest neighbor Ni^{2+}, the total spin Hamiltonian for the pair can be expressed as

$$H_T = H + H' + H_P \ , \tag{2.1}$$

where

$$H = g\mu_B \vec{S} \cdot \vec{H} + b_2^0 O_2^0 + b_2^2 O_2^2 + b_4^0 O_4^0 + b_4^2 O_4^2 + b_4^4 O_4^4$$

is the spin Hamiltonian of the Mn^{2+} ion ($S = \frac{5}{2}$) (see Sec. III for further details);

$$H' = g_1\mu_B \vec{S}_1 \cdot \vec{H} + \beta_2^0 O_2^0 + \beta_2^2 O_2^0$$

is the spin Hamiltonian of the Ni^{2+} ion ($S_1 = 1$), and $H_P = J\vec{S} \cdot \vec{S}_1$ represents the Ni^{2+}-Mn^{2+} exchange interaction, where *J* is the exchange-interaction constant.

The wave functions of the total system can thus be expressed as product wave functions $\psi_1(M)\psi_2(M')$, where $M = \pm\frac{5}{2}, \pm\frac{3}{2}, \pm\frac{1}{2}$, and $M' = \pm 1, 0$. Thus the spin Hamiltonian of the pair system is an 18×18 matrix. If we assume now that the external magnetic field is along the *z* axis, the following expressions can be obtained, using per-

turbation theory and neglecting smaller zero-order terms in the spin Hamiltonian of Mn^{2+}:

$$E(\pm\tfrac{1}{2},0) = \pm\tfrac{1}{2}g\mu_B H - \tfrac{8}{3}b_2^0 - \tfrac{2}{3}\beta_2^0 + 4J^2/(\mp g\mu_B H \pm g_1\mu_B H - 2b_2^0 - \beta_2^0) + \tfrac{9}{2}J^2/(\pm g\mu_B H \mp g_1\mu_B H - \beta_2^0) \ . \qquad (2.2)$$

From the above energy levels, using the resonance condition (for the transition $\tfrac{1}{2} \leftrightarrow -\tfrac{1}{2})h\nu = g_{obs}\mu_B H$, one obtains the following expression for the g factor as observed in a paramagnetic host lattice:

$$g_{obs} = g + J^2(g + g_1)/(\beta_2^0)^2 \ , \qquad (2.3)$$

where b_2^0 has been neglected, since $b_2^0 \ll \beta_2^0$.

From Eq. (2.3) it is clearly seen that from the observed g factor in a paramagnetic host lattice one can estimate the exchange constant between the host-guest paramagnetic ions if the values of the g factors for the guest (in isostructural diamagnetic lattice) and host paramagnetic ions and the zero-field splitting parameter for the host ions are known.

The value of $|J|$, using Eq. (2.3), as estimated in Sec. IV, turns out to be 5.88 GHz.

III. CRYSTAL STRUCTURE, SAMPLE PREPARATION, AND EXPERIMENTAL DETAILS

The ZPSH and NPSH crystals, like the other tutton salts, belong to the monoclinic symmetry, with space group $P2/a$ (C_{2h}^4). The unit cell contains two formula units. Six water molecules form an octahedron around the divalent metal ion. The unit-cell dimensions are $a = 8.98$, $b = 12.22$, and $c = 6.10$ Å, and the monoclinic angle β is about 105°. For more details see Ref. 2.

The single crystals of Mn^{2+}-doped ZPSH and NPSH were grown by slow evaporation at room temperature of solutions of ZPSH and NPSH, each containing 0.1% $MnSO_4 \cdot 6H_2O$ stoichiometrically. In order to avoid sample demagnetization effects at low temperatures, the spheres of 1–2 mm of NPSH samples were prepared by blowing the roughly cubic single crystals on emery paper.

The experimental arrangement is the same as that described in Ref. 2.

IV. SPIN HAMILTONIAN, DATA, AND EVALUATION OF PARAMETERS

The spin Hamiltonian appropriate to present samples of monoclinic symmetry is in standard notation[10]:

$$H = \mu_B \vec{H}\cdot\vec{g}\cdot\vec{S} + \sum_{m=0,2}\tfrac{1}{3}b_2^m O_2^m + \sum_{m=0,2,4}\tfrac{1}{60}b_4^m O_4^m$$

$$+ AS_z I_z + B(S_x I_x + S_y I_y) + Q'[I_z^2 - \tfrac{1}{3}I(I+1)]$$

$$+ Q''(I_x^2 - I_y^2) \ . \qquad (4.1)$$

Here $\vec{g}$, b_l^m, A, B, Q', and Q'' are the spin-Hamiltonian parameters, O_l^m are spin operators,[10] μ_B is the Bohr magneton, H is the external magnetic field, and S and I are the electron and nuclear spins, respectively $(S = I = \tfrac{5}{2})$.

The X, Y, and Z axes are chosen to coincide with the principal axes of the b_2^m tensor, so that the overall splitting of the spectra is maximum along the Z axis and minimum
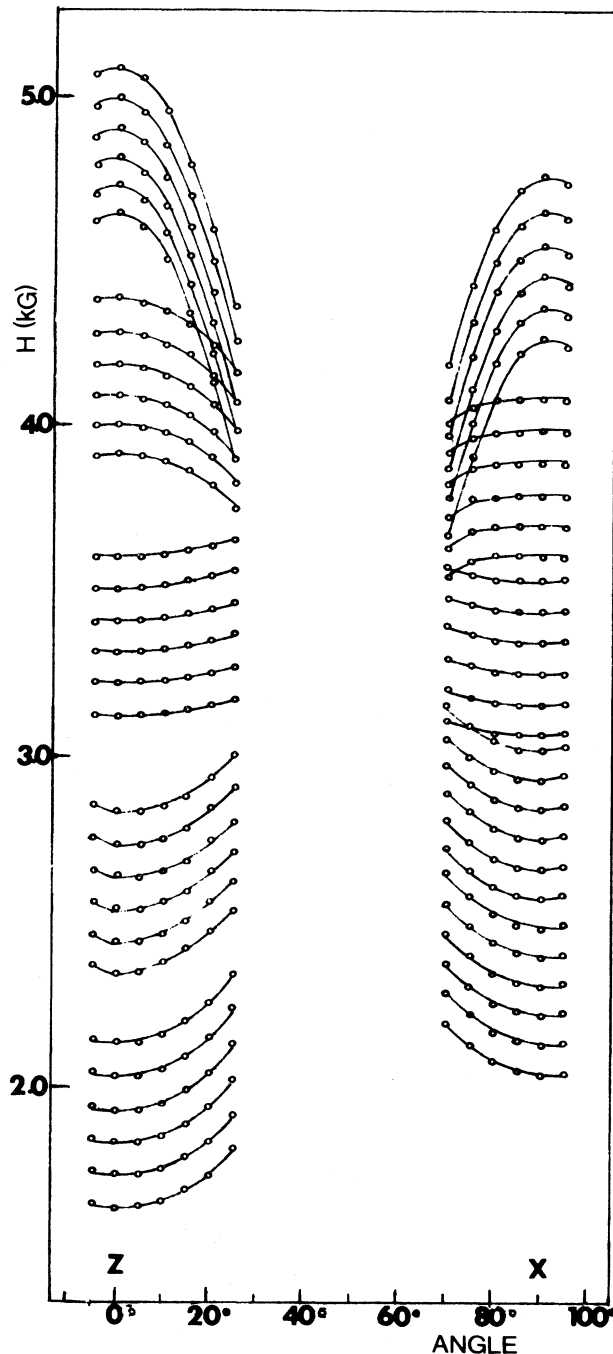
FIG. 1. Angular variation of X-band spectrum in the ZX plane for the Mn^{2+}-doped ZPSH host at room temperature. The circles represent the experimental resonant-line positions, and the solid lines are smooth curves that connect data points from the same transition. Only spectra corresponding to one inequivalent Mn^{2+} ion have been exhibited.

TABLE I. Values of spin-Hamiltonian parameters for the Mn^{2+}-doped ZPSH host (0.1%). RMS linewidth (RMSL) (in GHz) is $(\sum_j(|\Delta E_j| - h\nu_j)^2/n)^{1/2}$, where ΔE_j is the calculated energy difference between levels participating in resonance for the jth resonant magnetic field value, $h\nu_j$ is the energy of microwave radiation, and n is the number of points used in each fitting. The parameters b_l^m, Q', Q'', A, and B are expressed in units of GHz. A negative sign has been assumed for the value of A. The indicated errors are calculated by use of the statistical method (Ref. 12). The parameters at room temperature, as reported in Ref. 1, have also been included for comparison.

Temperature	295 K[a]	85 K[a]	5 K[a]	295 K[b]
g_{zz}	1.996 ± 0.001	2.001 ± 0.001	2.002 ± 0.001	2.016
g_{xx}	1.999 ± 0.001	2.021 ± 0.001	2.013 ± 0.001	2.016
b_2^0	-1.068 ± 0.002	-1.315 ± 0.002	-1.359 ± 0.002	0.730
b_2^2	0.504 ± 0.005	0.528 ± 0.005	0.489 ± 0.005	0.605
b_4^0	0.018 ± 0.001	0.019 ± 0.001	0.021 ± 0.001	...
b_4^2	-0.014 ± 0.023	0.002 ± 0.025	-0.225 ± 0.025	...
b_4^4	0.011 ± 0.023	0.047 ± 0.023	-0.133 ± 0.026	...
Q'	-0.021 ± 0.006	-0.015 ± 0.006	0.002 ± 0.006	0.004
Q''	-0.058 ± 0.011	-0.040 ± 0.001	0.015 ± 0.011	0.025
A	-0.265 ± 0.004	-0.259 ± 0.004	-0.258 ± 0.004	-0.244
B	-0.269 ± 0.004	-0.264 ± 0.004	-0.260 ± 0.004	-0.246
n	287	297	232	...
RMSL	0.028	0.031	0.052	...

[a]This work. [b]Reference 1.

along Y.[11] The spectra for ZPSH were recorded at room, liquid-nitrogen, and liquid-helium temperatures, while that of NPSH at room and liquid-helium temperatures only. The general shape of the spectra and angular variation of resonant-line positions with respect to the external magnetic field for the NPSH host are given in Ref. 2. For the ZPSH host two sets of spectra corresponding to two inequivalent Mn^{2+} ions in the unit cell were observed. For each, along their respective Z and X axes, 30 distinguishable hyperfine lines, plus some forbidden lines appearing mostly near the central fine transition $-\frac{1}{2} \leftrightarrow \frac{1}{2}$, were observed. Along the Y axis, the number of overlapped lines increased and only

24 lines appeared. The shape of the spectra remained the same at all temperatures; however, the overall splitting increased with lowering the temperature. The angular variation of spectra for ZPSH is shown in Fig. 1.

The parameters were evaluated by use of a rigorous least-squares fitting (LSF) procedure specifically designed and adapted to the electron-nuclear spin-coupled system of Mn^{2+}.[5] First, the fine-line positions were estimated to evaluate initial values of fine-structure parameters, and LSF fitting was used in the purely electronic space,[3] fitting simultaneously all estimated fine-line positions. This saved com-

TABLE II. Values of spin-Hamiltonian parameters of spherical sample for the Mn^{2+}-doped NPSH host (0.1%). Other details and notations are the same as those given in the caption of Table I.

Temperature	295 K	5 K	1.8 K
g_{zz}	2.058 ± 0.002	2.017 ± 0.002	2.024 ± 0.002
g_{xx}	2.025 ± 0.002	1.991 ± 0.002	1.974 ± 0.002
b_2^0	-0.750 ± 0.026	-1.198 ± 0.025	-1.260 ± 0.023
b_2^2	0.564 ± 0.025	0.432 ± 0.022	0.395 ± 0.021
b_4^0	0.300 ± 0.068	0.125 ± 0.083	0.111 ± 0.082
b_4^2	0.910 ± 0.236	0.454 ± 0.300	0.342 ± 0.300
b_4^4	0.153 ± 0.047	0.200 ± 0.079	0.125 ± 0.076
Q'	0.009 ± 0.001	0.001 ± 0.001	-0.001 ± 0.001
Q''	-0.003 ± 0.030	0.014 ± 0.030	0.042 ± 0.030
A	-0.275 ± 0.004	-0.115 ± 0.004	-0.169 ± 0.004
B	-0.232 ± 0.004	-0.228 ± 0.004	-0.228 ± 0.004
n	149	160	160
RMSL	0.052	0.036	0.043
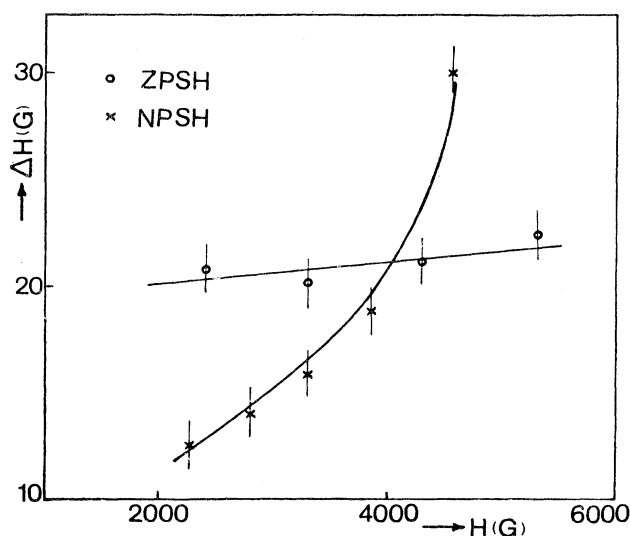
FIG. 2. Variation of linewidths as a function of magnetic field intensity at liquid-helium temperature for the orientation of the external magnetic field along the Z axis for the NPSH and ZPSH hosts.

puter time on the final fitting of all the hyperfine line positions on the LSF procedure, using the fine-structure parameter values, already obtained, as initial values.

The values of the parameters so obtained for ZPSH are significantly different from those reported in Ref. 1. The fourth-order parameters, neglected in Ref. 1, are found to have small, but significant values. The absolute sign of b_2^0, determined from relative intensities of lines at liquid-helium temperatures, is negative, since the intensity of the highest-field sextet *decreased* relative to that of the lowest-field sextet as the temperature was lowered to liquid-helium temperatures.[10] The values of parameters for the NPSH and ZPSH samples are given in Tables I and II at various temperatures. The errors were determined by use of a statistical method.[12]

From the observed g values of the spherical NPSH host at liquid-helium temperature and the g values for the ZPSH host, as given in Tables I and II, the value of J was found to be, using Eq. (2.3), $|J| = 5.88$ GHz. The values for the Ni^{2+} ion used were $g_1 = 2.25$ and $\beta_2^0 = 99$ GHz as found by Griffiths and Owen.[13]

V. LINEWIDTHS

The EPR linewidths for the ZPSH lattice were of the order of 20 G for all lines at all temperatures. On the other hand, for the NPSH host, the linewidths showed anisotropy with respect to the direction of the external field. Moreover, they depend upon the intensity of the external field also. These behaviors can be explained to be due to the presence of Ni^{2+} ions (see below). In particular, for the NPSH host, for the orientation of the external field along the Z axis, only a few lines at low magnetic fields were observed, the widths of the lines increased with increasing magnetic field intensity, and for sufficiently high magnetic field intensity all lines completely broadened out and disappeared. For the magnetic field along the X axis, the line broadening is not much, and all lines are observable.

As discussed in Ref. 2 the paramagnetic Ni^{2+} ions in the NPSH lattice are responsible for the different behaviors of linewidths in the NPSH and ZPSH lattices. This is due to the magnetic moment induced on the Ni^{2+} ions because of the presence of the external magnetic field, the moment depending upon the spin-Hamiltonian parameters g_1, β_2^0, and β_2^2 of Ni^{2+} in the NPSH lattice (for further details see Ref. 2).

The linewidth variation is shown in Fig. 2 as a function of field intensity.

[1]S. Kasthurirengan and R. R. Navalgund, Phys. Status Solidi (b) 72, K1 (1975).
[2]S. K. Misra and M. Jalochowski, Physica B 112, 83 (1982).
[3]S. K. Misra, J. Magn. Reson. 23, 403 (1976).
[4]C. Kittel, Phys. Rev. 73, 155 (1948).
[5]S. K. Misra, Physica B 121, 193 (1983).
[6]M. T. Hutchings and W. P. Wolf, Phys. Rev. Lett. 11, 187 (1963).
[7]M. T. Hutchings, C. G. Windsor, and W. P. Wolf, Phys. Rev. 148, 444 (1966).
[8]M. R. St. John and R. J. Myers, Phys. Rev. B 13, 1006 (1976).
[9]W. T. Batchelder, Ph.D. thesis (University of California, Berkeley, 1970) (unpublished).
[10]A. Abragam and B. Bleaney, *Electron Paramagnetic Resonance of Transition Ions* (Clarendon, Oxford, 1970).
[11]M. Weger and W. Low, Phys. Rev. 111, 1526 (1958).
[12]S. K. Misra and S. Subramanian, J. Phys. C 15, 7199 (1982).
[13]J. H. E. Griffiths and J. Owen, Proc. R. Soc. London, Ser. A 213, 459 (1952).